References

BERGFEST A., 1955. Bacúch, Manuscript, Geofond, Bratislava, Slovakia (in Slovak).

BIELY A. (eds.), 1992. Geological map of the Nízke Tatry Mountains 1:50,000. GS SR, Bratislava (in Slovak with English summary).

BROWN P.E., 1989. Flincor: A microcomputer program for the reduction and investigation of fluid inclusion data. *Am. Mineralogist*, 74: 1390-1393.

ČERNYŠEV I., CAMBEL B. and KODĚRA M., 1984. Lead isotopes in galenas of the West Carpathians. *Geol. Zbor. Geol. Carpath.*, 35 (3), 307-327.

ĎUĎA R., 1996. Slovak minerals. New knowledge from the years 1980–1995. *Natura carpathica*, 37: 9-52 (in Slovak).

GRECULA P. (ed.), 1995. Mineral deposits of Slovak Ore Mountain, v.1., Bratislava, (in Slovak with English summary).

HAK J. and LOSERT J., 1962. About the post-Werfenian ore mineralization nearby Trangoška in the Nízke Tatry Mts. Sbor. UNS, Kutná Hora, Praha, 57-120 (in Czech).

HURAI V., GAZDAČKO Ľ., FERENČÍKOVÁ E., MAJZLAN J. and REPČOK I., 1998. Origin of ore-bearing fluids of veins siderite deposits Gretla, Jedľovec and Rudňany (Slovak Ore Mountain) Min., Slov., 30, 423-430. (in Slovak with English summary).

HVO•ĎARA P., 1971. Research of gold-bearing mineralization of some core mountains of Western Carpathian, Manuscript, Geofond, Bratislava, Slovakia (in Slovak).

CHOVAN M., PUTIŠ M., NÉMETH Z., MA•O Ľ., ANDRÁŠ P. and JELEŇ S., 1999. Gold-hosted mineralizations in the Western Carpathians, paleotectonic position, Min. Slov. 31, 3-4, 175-178 (in Slovak).

IRÓ S., 1996. Genetical model of Fe-Mg carbonate mineralization of Gemeric and Veporic Units. PhD. Thesis, PrifUK, Bratislava, Slovakia (in Slovak).

ILAVSKÝ J., 1986. Mineral deposits of the Czechoslovak Carpathians. In: DUNNING F.W. and EVANS A.M., (Editors), Mineral deposits of Europe. Vol. 3: Central Europe. Inst. Mining Metall. and Min. Soc., London, pp. 146-173.

KANTOR J. and RYBÁR M., 1964. Isotope of lead from several deposits of West Carpathian crystalline. *Geol. Sbor. Slov. Akad. Vied*, 15 (2), 285-297.

KODĚRA M. ed., 1986–1990. Topographic mineralogy of Slovakia I-III, Veda, Bratislava (in Slovak).

KOTOV A.B., MIKO O., PUTIŠ M., KORIKOVSKIJ S.P., BEREZNAYA N.G., KRÁĽ J. and KRIST E., 1996. U/Pb dating of zircons of petrogenetic acid metavolcanics and metasubvolcanics: A record of Permian–Triassic taphrogeny of the West-Carpatian basement. *Geol. Carpath.*, 47 (2), 73-79.

KUPČÍK V., SCHNEIDER A. and VARČEK C., 1969. Chemismus von einigen Bi-sulfosalzen aus dem Zips-Gömörer Erzgebirge (CSSR). *Neues Jb. Miner. Mh.*, 10, 445-454.

MAJZLAN J. and OZDÍN D., 1995. Cu-Pb-Bi sulphosalts from Nízke Tatry Mts. *Min. Slov.*, 27 (4), 290-292 (in Slovak).

MAKOVICKÝ E., 1977. Chemistry and crystallography of the lillianite homologous series. Part III. Crystal chemistry of lillianites homologues, Related phases, *N. Jb. Miner. Abh*, 131: 187-207

MAKOVICKÝ E., 1989. Modular classification of sulphosalts - current status. Definition and application of homologous series. *N. Jb. Miner. Abh*, 160 (3), 269-297.

MAKOVICKÝ E. and KARUP-MŘLLER S., 1977a. Chemistry and crystallography of the lillianite homologous series. Part I: General properties and definitions. *N. JB. Miner. Abh*, 130: 264-287.

MAKOVICKÝ E. and KARUP-MŘLLER S., 1977a. Chemistry and crystallography of the lillianite homologous series. Part II: Definition of new minerals: eskimoite, vikingite, ourayite and treasurite. redefinition of schirmerite and new data on the lillianite – gustavite solid – solution series. *N. Jb. Miner. Abh.*, 161: 56-82.

MIKO O. and KORIKOVSKIJ S. P., 1993. Metamorphism of the Jánov Grúň Lower paleozoic volcano-sedimentary formation (Veporic Unit, Western Carpathians), *Geologica Carpathica*, 45 (1), 57-65.

OZDÍN D. and CHOVAN M., 1999. New mineralogical and paragenetic knowledge about siderite veins in the vicinity of Vyšná Boca, Nízke Tatry Mts., *Slov. Geol. Mag.*, 5 (4), 255-271.

PETRO M., 1973. Mineral raw material at the sheet Polomka 1:25,000, MS, Geofond, Bratislava, Slovakia (in Slovak).

PETRO M., 1976. Metalogenesis of Veporic Unit., MS, Geofond, Bratislava, Slovakia (in Slovak).

PROCHASKA W., 1998. Significance of fluid chemistry for the origin of siderite mineralization in the Greywacke zone of the Eastern Alps. Carpathian-Balkan Geological Association XVI Congress, Vienna, Austria, p.494.

SLAVKAY M. and PETRO M., 1993. Metalogenesis and ore formation of Veporic Unit. *Miner. Slov.*, 25 (5), 313-317 (in Slovak with English summary).

SPRINGER G., 1971. The synthetic solid-solution series Bi_2S_3-$CuPbBiS_3$ (bismuthinite-aikinite). N. Jb. Miner. Monatsh 1971, 19-27.

Early Paleozoic Manganese Ores in the Gemericum Superunit Western Carpathians, Slovakia

Igor ROJKOVIČ

Faculty of Natural Sciences, Comenius University, Bratislava, Slovakia

ABSTRACT: Stratiform manganese ores are bound to the metamorphosed Early Paleozoic black shale of the Gemericum Superunit. Sedimentary – diagenetic manganese accumulation is overlapped by the association of the metamorphic minerals due to the Hercynian metamorphism. Rhodonite, rhodochrosite, anthophyllite, chlorite, quartz, Mn-rich calcite, magnetite, pyroxmangite, pyrophanite, spessartite and tephroite represent metamorphosed manganese carbonate-silicate rock (queluzite). Pyrite, chalcopyrite, cobaltite, pyrrhotite, galena, pentlandite, sphalerite, ullmannite, calcite and quartz represent the younger hydrothermal phase of mineralization. Pyrolusite, todorokite, cryptomelane and iron hydroxides were formed in the oxidation zone.

KEY WORDS: manganese ore, mineral associations, metamorphism, Slovakia.

Introduction

Occurrences of the manganese ore are bound to the Early Paleozoic black phyllites and lydites of the Gemericum Superunit, 2 km NNE from Čučma village on the western slope of Stredná Hora hill and 4 km to NW from Smolník in Bystrý Potok valley on NW slope of Malá Hekerová hill (Fig. 1). Lenses of manganese ore from 50 to 100 m long and up to 4 m thick are conformable to wall rocks (Fig. 2). Several thousands tons of oxidized ore were mined at the deposit (Papp 1915 in Grecula et al. 1995). Rhodonite accompanied by rhodochrosite, quartz, magnetite, garnet, tremolite, pyrite and accessory chalcopyrite, arsenopyrite, alabandite, galena and barite were known during the time of exploitation (between 19th and 20th century). Manganese ore was replaced by the mixture of pyrolusite, "psilomelane", manganite and "wad" with "limonite" in oxidation zone (Maderspach 1880; Papp 1915). Mn-rich calcite, calcite, Mn-rich tremolite, spessartite, accessory pyrrhotite, marcasite, sphalerite, hematite, muscovite, chlorite-group mineral, bementite (?) and apatite group mineral were identified later by Kantor (1954). Mn-rich fayalite ("knebelite"), manganpyrosmalite, pyrophanite, biotite-like mica, "phengite", and "caryopilite" and Mn-rich actinolite instead of bementite and Mn-rich tremolite (Kantor 1954), were identified by Faryad (1994).

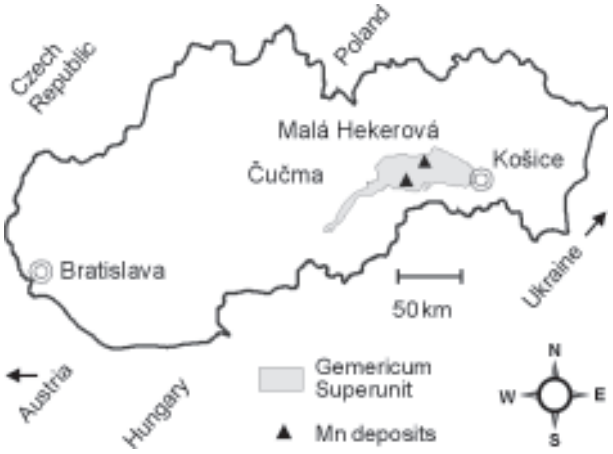

Fig. 1. Localization of the Čučma and Malá Hekerová deposits in the Gemericum Superunit.

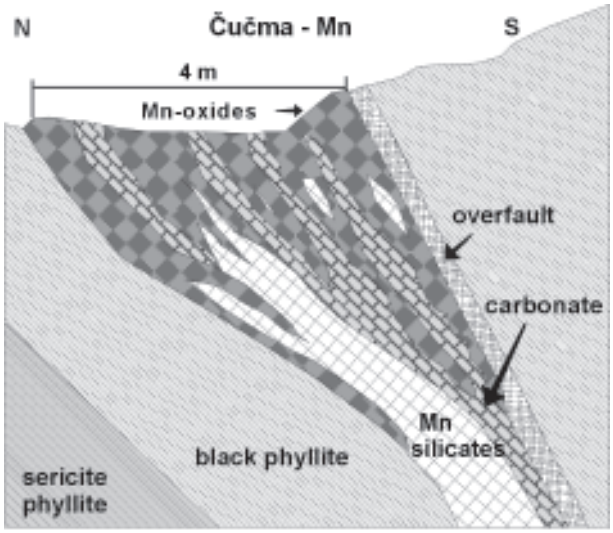

Adapted according to Maderspach and Schafarik (in Grecula et al. 1995)

Fig. 2. Geological cross-section of the Čučma deposit.

Kantor (1954) presumed syngenetic origin of manganese mineralization related to basic volcanism of the Gelnica Group accompanied by metasomatic replacement of limestone. Origin of ore was related to volcano-sedimentary activity as well as to reduction environment of black shale, accompanied by formation of limestone, Mn and Fe-bearing carbonates, sulphides and silica gel according to Grecula et al. (1995).

Methods

A wave-dispersion X-ray microanalysis (WDX) by JEOL-733 SUPERPROBE and an energy-dispersion X-ray microanalysis (EDX) by KEVEX were used for analysis of chemical composition of minerals. The accelerating voltage for WDX analysis was 15 kV, the beam current 11–12 nA or 15–18 nA and the counting time 20 sec. Natural and synthetic standards were used for calibration, and a ZAF correction procedure was employed. Al_2O_3, $BaSO_4$, wollastonite, CeO_2, NaCl, chromite, hematite, orthoclase, LaB_6, MgO, rhodonite, albite, Nd_2O_3, $PrPO_4$, SiO_2, $SrTiO_3$ and TiO_2 were used as standards for analysing of oxide and silicate minerals. Arsenopyrite, native Co, chalcopyrite, native Ni, Sb and Zn were used for sulphides. Chemical composition was calculated according to the Minfile programme.

X-ray diffraction analysis (XRD) was made on a Philips PW 1710 diffractometer. Samples with high content of Fe were analysed by Co K_α radiation ($\lambda\alpha_1$ = 1.78896 m^{-10}, $\lambda\alpha_2$ = = 1.79285 m^{-10}) and Cu Ka radiation ($\lambda\alpha_1$ = 1.54060 m^{-10}, $\lambda\alpha_2$ = = 1.54439 m^{-10}) was used in case of other samples. Accelerating voltage of 35 kV and beam current of 20 mA were used in the range 4-60 ° 2Θ with shift 0.02 ° 2Θ.

Results

Dominant minerals of manganese ore are rhodonite, Ca-rich rhodochrosite and Mn-rich calcite. Frequent are tephroite, antophyllite, pyroxmangite, quartz, todorokite and Fe-hydroxides (the last two mostly on the surface of samples). Less abundant are chlorite group mineral, magnetite, pyrolusite, pyrite, pyrrhotite, pyrophanite (Fe-rich) and goethite. Rare are Manganpyrosmalite, bementite, muscovite, chalcopyrite, galena, sphalerite, pentlandite, albite, rutile, cryptomelane and fluorapatite. Accessory minerals are ullmannite, cobaltite and allanite-(Ce).

Rhodonite $(Mn^{2+},Fe^{2+},Mg,Ca)SiO^3$ is dominant mineral of the fresh samples. Elongated grains from 0.5 to 1 mm long (rarely up to 2 cm long crystals) can be observed, locally with distinct cleavage parallel to elongation of grains (Fig. 3). Quartz, car-

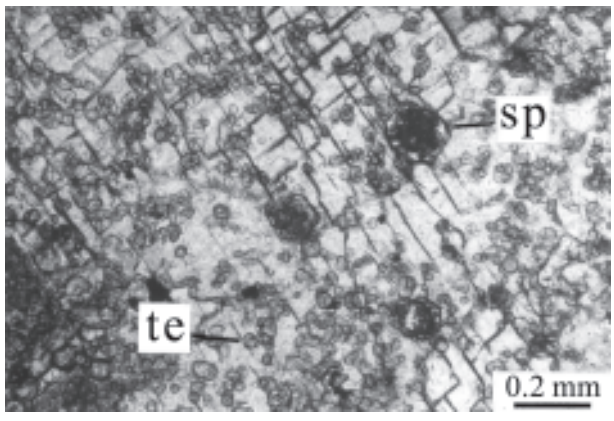

Fig. 3. Small tephroite grains (te) and spessartite (sp) crystals in rhodonite with distinct cleavage (white). Čú 2, transmitted light, parallel polar.

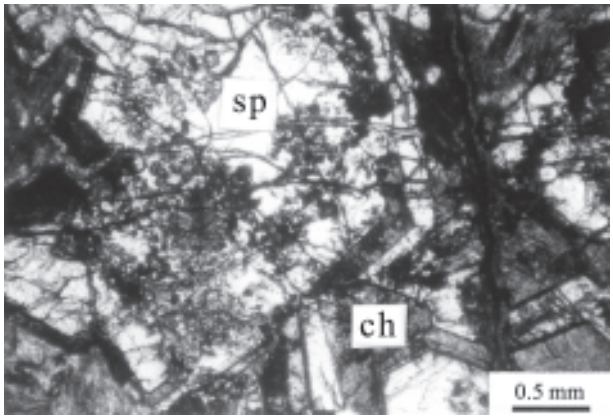

Fig. 4. Spessartite crystals (sp) replaced and cut by chamosite (ch). Ču 21, transmitted light, parallel polar.

bonates and chlorite veinlets fill grains along the cleavage and crossing fissures. **Pyroxmangite** $(Mn^{2+},Fe^{2+})SiO^3$ shows twinning lamellae. Elongated columnar crystals with less distinct cleavage are disseminated and form aggregates up to 2.5 mm across. It is overgrown and cut by carbonate veinlets. It is more frequent in carbonate rich parts. **Spessartite** $Mn^{2+}{}_3Al_2(SiO_4)_3$ euhedral grains (0.1 to 0.5 mm in size) form clusters and aggregates in rhodonite and Ca-rich rhodochrosite (up to 5 mm across). Small relics of Ca-rich rhodochrosite can be observed in their cores. They are replaced and cut by veinlets of younger carbonate and chlorite (Fig. 4). **Tephroite** $Mn_2{}^{2+}(SiO_4)$ grains (mostly 0.1 to 0.2 mm in size) and hypidiomorphic aggregates are closely associated with rhodonite. Faryad (1994) found "knebelite" (Mn-rich fayalite). Chemical composition with dominant Mn confirms tephroite member of fayalite-tephroite series (Redfern et al. 1998, Tab. 1, Fig. 5). **Anthophyllite** $Mg_7Si_8O_{22}(OH)_2$ forms prismatic crystals with rhombic sections (up to 4 mm long) in rhodonite and carbonate (Fig. 6). Previous studies have found Mn-rich tremolite (Kantor 1954), "tirodite" and actinolite

	rhodonite	pyrox--mangite	tephroite	bementite	mangan-pyrosmalite
			Weight %		
SiO_2	46.250	46.180	30.770	33.830	33.880
$Al2O_3$	0.420	0.290		1.430	
FeO	3.910	8.270	10.580	27.560	3.010
MnO	44.770	41.240	59.400	25.390	49.130
MgO	0.680	1.120		0.800	
CaO	3.600	3.400			
Cl					2.800
Total	99.630	100.480	100.750	89.010	88.820
			Atomic proportion		
Si	0.996	0.990	1.020	5.837	6.056
Al	0.010	0.007		0.288	
Fe^{+2}	0.071	0.148	0.293	3.974	0.450
Mn^{+2}	0.817	0.748	1.667	3.712	7.439
Mg	0.022	0.036		0.206	
Ca	0.083	0.078			
Total	1.999	2.007	2.980	14.018	13.944
Cl					0.847
O	3.000	3.000	4.000	20.000	20.000

Tab. 1. Chemical composition of Mn-silicate minerals from Čučma and Malá Hekerová deposits.

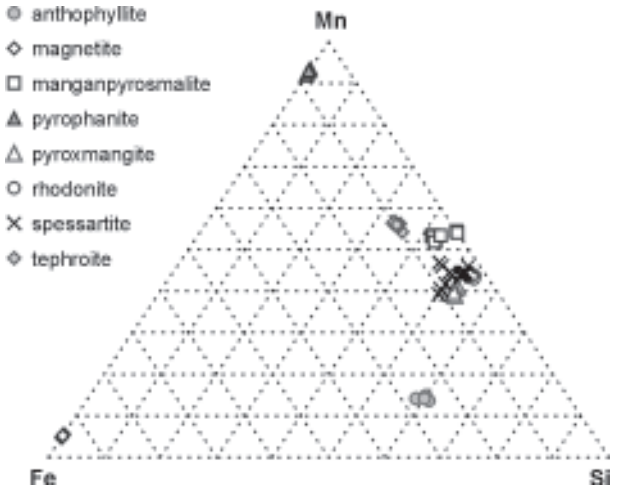

Fig. 5. Mn-Fe-Si composition of minerals from Čučma and Malá Hekerová deposits.

(Faryad 1994). Studied hornblende shows Fe-Mn-Mg composition and X-ray diffraction peaks correspond to antophyllite (Tab. 2, Fig. 7). **Manganpyrosmalite** $(Mn^{2+},Fe^{2+})_8Si_6O_{15}(OH,Cl)_{10}$ forms rare disseminated grains (up to 0,02 mm in size). It was found in association with rhodonite, tephroite, pyrophanite and magnetite. **Bementite** $Mn_8Si_6O_{15}(OH)_{10}$ forms veinlets (up to 0.5 mm thick) and rims

spessartite		antophyllite		chamosite		muscovite	
			Weight %				
SiO_2	36.12	SiO_2	50.49	SiO_2	31.63	SiO_2	46.03
TiO_2	0.18					TiO_2	0.37
Al_2O_3	16.32	Al_2O_3	0.29	Al_2O_3	15.90	Al_2O_3	32.43
Cr_2O_3	0.14						
Fe_2O_3	5.93	FeO	23.55	FeO	26.57	FeO	2.00
MnO	36.78	MnO	14.93	MnO	2.57	K_2O	10.23
MgO	0.11	MgO	7.56	MgO	8.70	MgO	1.87
CaO	4.89	CaO	0.56	CaO	0.33	Na_2O	0.47
		H_2O*	1.09	H_2O*	11.43	H_2O*	4.50
Total	100.45	Total	99.27	Total	97.12	Total	97.89
			Atomic proportion				
Si IV	5. 988	Si IV	7. 968	Si IV	3. 417	Si IV	6. 273
Al IV	0. 012	Al IV	0. 021	Al IV	0. 583	Al IV	1. 727
T site	**6. 000**	**T site**	**7. 989**	**T site**	**4. 000**	**T site**	**8. 000**
Al VI	3. 177	Al VI	0. 033	Al VI	1. 453	Al VI	3. 483
Ti VI	0. 022						
Cr	0. 018	Fe^{+2}	3. 108	Fe^{+2}	2. 413	Fe^{+2}	0. 230
Fe^{+3}	0. 739	Mn	0. 081	Mn	0. 237	Ti VI	0. 040
		Mg	1. 776	Mg	1. 417	Mg	0. 380
				Ca	0. 040		
O site	**3. 956**	**M123**	**5. 000**	**O site**	**5. 560**	**O site**	**4. 133**
Mn^{+2}	5. 165	Mn	1. 914			Na	0. 127
Mg	0. 028	Ca	0. 065			K	1. 780
Ca	0. 868	M4 site	1. 980				
		Ca	0. 031				
A site	**6. 061**	**A site**	**0. 031**			**A site**	**1. 907**
O	24. 000	O	22. 000	O	9. 727	O	19. 910
		OH	2. 000	OH	8. 273	OH	4. 090

*- calculated according to the Minfile programme

Tab. 2. Chemical composition of silicate minerals from Čučma and Malá Hekerová deposits.

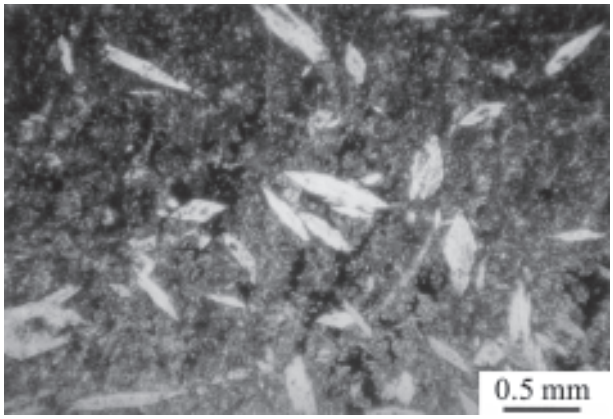

Fig. 6. Antophyllite crystals (white) in rhodonite (grey). Čú 12, transmitted light, parallel polar.

	rhodochrosite	calcite
	Weight %	
FeO	1. 10	2. 20
MnO	51. 25	11. 60
MgO	0. 55	0. 66
CaO	5. 40	41. 35
CO_2*	37. 40	41. 68
Total	95. 70	97. 49
	Atomic proportion	
Fe	0. 018	0. 033
Mn	0. 849	0. 174
Mg	0. 016	0. 017
Ca	0. 117	0. 776
CO_3	1. 000	1. 000

*- calculated according to the Minfile programme

Tab. 3. Chemical composition of carbonates from Čučma and Malá Hekerová deposits.

on spessartite. Chemical composition with low Al content excludes a chlorite-group mineral and may correspond to "caryopilite" identified by Faryad (1994). **Chamosite** $(Fe,Al,Mg)_{4-6}(Si,Al)_4O_{10}(OH)_8$, forms veinlets (up to 0.5 mm thick) with sulphides, cutting rhodonite, spessartite as well as carbonate veinlets. Chemical composition corresponds to chamosite. **Muscovite** KAl_2 ?$AlSi_3O_{10}$ $(OH)_2$ – crystals (0.5 to 1 mm in size) are disseminated in rhodochrosite or form veinlets in rhodochrosite. **Albite** $Na[AlSi_3O_8]$ – grains with twinning lamellae (up to 0.5 mm in size) overgrow rhodonite. **Allanite–(Ce)** $(Ce,Ca,Y)_2(Al,Fe^{2+},Fe^{3+})_3(SiO_4)_3(OH)$ – small crystals (up to 0.01 mm across) were found associated with Mn-silicates. **Quartz** SiO_2 – anhedral grains (mostly 0.1 to 2 mm in size) form aggregates of mosaic texture and thin strips (up to 5 mm thick). Part of grains is recrystallized and oriented. Younger veinlets of quartz (0.02 to 1 mm thick) with anhedral grains cut aggregates of older recrystallized quartz with elongated oriented grains. It cuts rhodonite, Ca-rich rhodochrosite and spessartite. Thin quartz veinlets cut also older veinlets of quartz.

Rhodochrosite $Mn^{2+}CO_3$, is dominant in some samples. Aggregates of xenomorphic grains (0.1 to 0.2 mm, rarely up to 4 mm across) are overgrown and cut by coarser grained and more transparent Mn-rich calcite. It is often accompanied by quartz intergrowns. Chemical composition of rhodochrosite shows increased Ca content (up to 10 wt.% of CaO, Tab. 3). **Mn-rich calcite** $CaCO_3$ forms veinlets (0.1 to 0.2 mm thick) which cut older carbonates, rhodonite, spessartite and tephroite (Fig. 8). It is accompanied with quartz and pyrite. Several generations of carbonate veinlets can be observed, cutting each other and cut by younger quartz veinlets. MnO content in Mn-rich calcite ranges from 8 to 17 wt. %.

Magnetite $Fe^{+2}Fe^{+3}{}_2O_4$ forms isometric grains (0.02 to 0.1 mm across), which are disseminated in Mn-silicates and carbonates, and they often fill their intergranular space. Pyrophanite and pyrite enclose them. Magnetite aggregates (several cm in size), are cut by carbonate veinlets. Chemical composition of magnetite shows increased content of MnO ranging from 4.4 to 5.3 wt.%. **Pyrophanite** $Mn^{2+}TiO_3$ forms tabular crystals (up

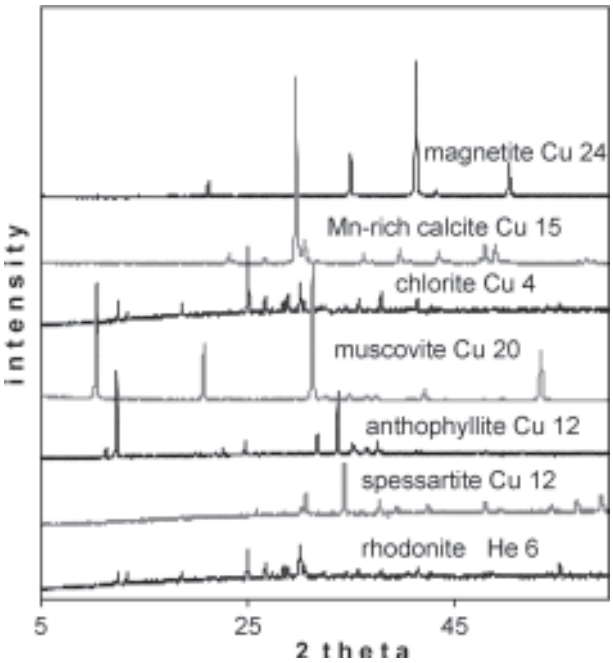

Fig. 7. X-ray diffraction analyses of minerals from Čučma and Malá Hekerová deposits.

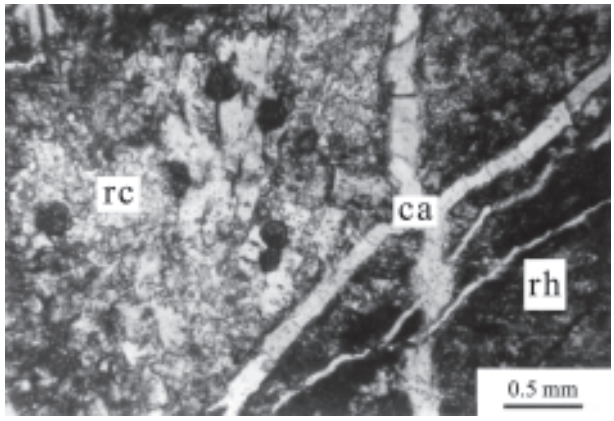

Fig. 8. Mn-rich calcite veinlets (ca) cut rhodonite (rh) and rhodochrosite (rc). Čú 5, transmitted light, parallel polar.

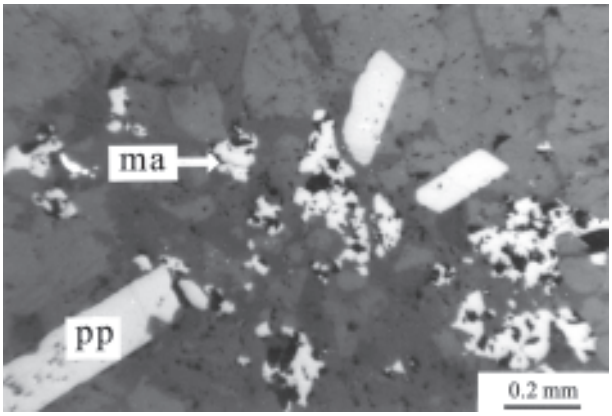

Fig. 9. Pyrophanite crystals (pp) and magnetite grains (ma) in the manganese-rich rock. Ču 1, reflected light, parallel polar.

to 0.5 mm in size), brownish-grey in reflected light with distinct bireflection, anisotropy and red internal reflection (Fig. 9). It encloses older magnetite grains and it is enclosed by younger pyrite. **Fe-rich pyrophanite** $(Fe^{2+},Mn^{2+})TiO^3$ occurs as tabular crystals (up to 0.1 mm in size), associated with iron hydroxides. Fe-pyrophanite shows increased FeO content (close to 17 wt.%) in comparison to pyrophanite (Tab. 4). Stable atomic Mn/Fe ratio in analysed grains does not suggest a mixture of iron hydroxides and pyrophanite. **Rutile** TiO_2 forms prismatic crystals (up to 0.1 mm long) are oriented in parallel strips.

Todorokite $?(Mn^{+2},Ca,Mg)Mn^{+4}{}_3O_7.\ H_2O$, forms crusts and fissure fillings in manganese rocks, consisting of irregular and elongated grains (0.01 to 0.1 mm in size). Total of oxides (up to 90%) confirms manganese hydroxide. Absence of Ba excludes romanechite (Tab. 5). Presence of Ca and less distinct peaks of XDA indicate the presence of todorokite. **Cryptomelane** $?\ K_{<2}(Mn^{+4},Mn^{+2})_8O_{16}$, forms irregular and rounded grains in todorokite (0.02 to 0.05 mm across) and colloform aggregates. It shows higher relief, increased content of K and higher total of oxides comparing to todorokite. **Pyrolusite** $Mn^{4+}O_2$, elongated

	pyrophanite	Fe- rich pyrophanite	magnetite
		Weight %	
SiO_2	0. 160	0. 430	0. 050
TiO_2	52. 290	52. 140	0. 200
Fe_2O_3*			69. 640
FeO	3. 530	16. 800	26. 910
MnO	43. 740	30. 120	4. 870
Total	99. 720	99. 490	101. 670
Atomic proportion			
Si	0. 003	0. 011	0. 002
Ti	0. 992	0. 990	0. 006
Fe^{+3}			1. 985
Fe^{+2}	0. 074	0. 354	0. 849
Mn	0. 934	0. 644	0. 156
Mn,Fe^{+2}	1. 008	0. 998	1. 005
Total	2. 003	1. 999	2. 998
O	3. 000	3. 000	4. 000

*- calculated according to the Minfile programme

Tab. 4. Chemical composition of oxides from Čučma and Malá Hekerová deposits.

	pyrolusite	Todorokite	Cryptomelane
		Weight %	
SiO2	0. 450	0. 860	0. 300
MnO2	97. 650	84. 590	96. 300
Fe2O3	1. 050	3. 200	
CaO	0. 490	1. 150	0. 170
K2O			0. 870
Total	99. 640	89. 800	97. 640
		Atomic proportion	
Si	0. 011	0. 014	0. 005
Mn	0. 978	0. 944	0. 990
Fe	0. 011	0. 039	
Ca	0. 011	0. 020	0. 002
K			0. 016
Total	1. 011	1. 017	1. 013
O	2. 000	2. 000	2. 000

Tab. 5. Chemical composition of secondary Mn-oxides from Čučma and Malá Hekerová deposits.

grains (0.02 to 0.04 mm long) form aggregates (up to 0.7 mm in size) and veinlets (0.02 to 0.1 mm thick). It replaces and cuts todorokite aggregates with synaeresis cracks. XDA of weathered manganese rocks confirmed less distinct peaks of pyrolusite. **Goethite** α-$Fe^{+3}O(OH)$ form crusts of colloform zonal aggregates as well as fissure and intrergranular fillings. Chemical composition shows up to 1.5 wt.% of MnO_2.

Pyrite FeS_2 forms cubic crystals (0.01 to 0.3 mm across) are disseminated in rock. Subhedral and anhedral grains fill intergranular space of rock-forming minerals. Pyrite encloses, cuts and rims Mn–silicates, magnetite and pyrophanite. It is replaced, enclosed and cut by veinlets of pyrrhotite, sphalerite and chalcopyrite. **Pentlandite** $(Fe,Ni)_9S_8$ – forms admixtures in pyrrhotite (up to 0.06 mm long). **Pyrrhotite** $Fe_{1-x}S$ – forms veinlets and aggregates (up to 1 mm in size). It encloses, overgrows and cuts pentlandite, sphalerite, antophyllite and carbonate veinlets (Fig.

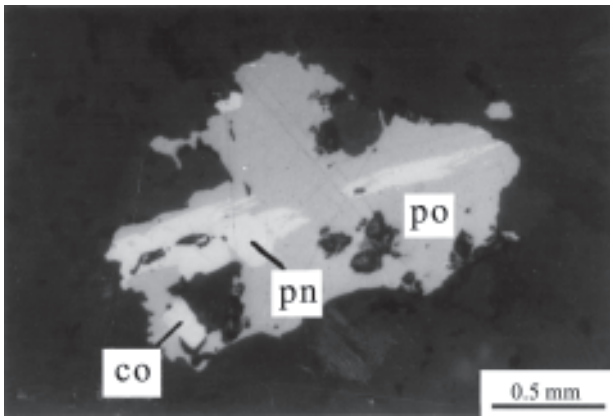

Fig. 10. Cobaltite (co) and pentlandite (pn) in pyrrhotite (po). Ču 1, reflected light, parallel polar.

10). It intergrows with chalcopyrite, bementite and it forms inclusions in pyrite. **Ullmannite** NiSbS, euhedral grains (0,01 to 0,4 mm across) are enclosed in pyrrhotite. **Galena** PbS, occurs as grains (up to 0.4 mm across) in quartz veinlets. They are accompanied by chalcopyrite, sphalerite and pyrite. **Cobaltite** CoAsS forms euhedral grains (0.05 mm in size) which are over-

	cobaltite	pentlandite	pyrrhotite	ullmannite
		Weight %		
Co	29. 880	2. 430		0. 590
Ni	3. 270	33. 360	0. 400	27. 300
Fe	2. 440	30. 810	59. 910	0. 750
As	45. 070			1. 030
Sb				56. 000
S	19. 160	33. 480	39. 690	14. 080
Total	99. 820	100. 070	100. 000	99. 750
		Atomic proportion		
Co	0. 843	0. 317		0. 022
Ni	0. 092	4. 380	0. 006	0. 996
Fe	0. 072	4. 252	0. 926	0. 029
As	1. 000			0. 030
Sb				0. 985
S	0. 993	8. 050	1. 068	0. 940
Total	3. 000	17. 000	2. 000	3. 000

Tab. 6. Chemical composition of Co-Ni-Fe-(Sb) sulphides from Čučma and Malá Hekerová deposits.

grown and enclosed in pyrrhotite and chalcopyrite. Results of chemical composition show increased contents of Fe (up to 13.3 wt.%) and Ni (up to 7.6 wt.%, Tab. 6). **Chalcopyrite** $CuFeS_2$, forms aggregates of anhedral grains (up to 0.5 mm across) and thin veinlets. It intergrows with pyrrhotite, encloses and overgrows cobaltite and sphalerite. **Sphalerite** (Zn,Fe)S occurs as disseminated grains (0.01 to 0.3 mm in size) and thin veinlets in association with quartz, pyrrhotite, galena, pyrite and chalcopyrite. It has increased Fe content (over 6 wt. % of Fe).

Based on detailed mineralogical study, the following three association of minerals were distinguished:

1) metamorphic,
2) hydrothermal,
3) supergene.

The first association of minerals was formed during metamorphism of the original sedimentary – diagenetic manganese ore, consisting most probably of Mn-rich carbonates, clay minerals and quartz. Disseminated sulphides are characteristic for the younger hydrothermal association. Weathering processes have resulted in the formation of manganese and iron oxides and hydroxides. The associations are following:

(1) metamorphic association: rhodonite, rhodochrosite, tephroite, spessartite, anthophyllite, pyroxmangite, magnetite, pyrophanite, muscovite, manganpyrosmalite, albite, rutile, allanite-(Ce),
(2) hydrothermal association: Mn-rich calcite, pyrite, pentlandite, sphalerite, chalcopyrite, pyrrhotite, cobaltite, ullmannite, galena, chamosite, bementite, quartz,
(3) supergene association: todorokite, pyrolusite, cryptomelane, goethite and "limonite".

Discussion

The Early Palaeozoic black phyllites and lydites of the Gemericum Superunit are rich in organic matter and represent metamorphosed black shales. The metamorphosed black sediments with the highest content of Corg (up to 20 wt. %) are accompanied by increased content of Au, Cu, Mo, S, Sb, U and V indicating euxinic environment of sedimentation (Rojkovič and Khun 1997). However, manganese is concentrated in the black phyllites with lower content of Corg and increased contents of K, Al, Th, La, Ti, Ba, Cr and B present in clastic or clay minerals (Rojkovič et al. 1995). Manganese was transported by ocean currents from the deep anoxic part of the stratified ocean into the margins of black shale facies where it mixed with shallower oxygen-bearing water with low manganese solubility and Mn oxides/hydroxides precipitated (Force and Cannon 1988). The manganese deposits may have formed by diagenetic processes analogous to deposits in the Black Sea (Roy 1992) and the Baltic Sea (Huckriede and Meischner 1996). Mn carbonates were formed from pore water system due to reduction of precipitated MnO_2 coupled with organic matter oxidation and microbial suboxic diagenesis (Okita 1992; Öztürk and Frakes 1995; Öztürk and Hein 1997; Gutzmer and Beukes 1998; Tang and Liu 1999). Other authors relate the origin of these deposits to volcanic activity (Fan et al.1992 in Öztürk and Hein 1997; Polgári 1993 in Öztürk and Hein 1997, Tang and Liu 1999). Manganese accumulations can be superimposed on the global geochemical record of sea-level changes reflecting the changes in global climates, the main transgressive phases and periods of increasing subsidence rate (Corbin et al. 2000). The manganese deposits modified by diagenesis occur in continental-margin areas of the oceans in shallow parts of the seas or the lakes. They generally show much higher Mn/Fe, Mn/Co, Mn/Ni, Mn/Cu and Mn/Pb ratios compared to the deposits in open oceans (Roy 1980).

Primary calcite may have been replaced by rhodochrosite during diagenesis of the Early Paleozoic manganese deposits in the Gemericum Superunit in the same way as in the Eocene deposits of Black Sea (Öztürk and Frakes 1995). High Mn/Fe ratio indicates diagenetic modification involving active role of organic matter in reduction environment. Metamorphosed manganese carbonate-silicate rock (queluzite), is characterized by the presence of Mn-carbonate and tephroite and general absence of lower oxides, particularly bixbyite. Queluzite originally consisted mainly of manganese carbonate, clay and silica (Roy 1980). The studied carbonate-silicate rocks of the Gemericum Superunit correspond to the queluzite type of metamorphosed manganese rock.

Association of metamorphic minerals overlaps sedimentary – diagenetic manganese accumulation formed in reduction environment. Relics of rhodochrosite can be locally seen in cores of some spessartites. Metamorphosed manganese rocks are represented mainly by rhodonite, tephroite, spessartite, rhodochrosite and Mn-rich magnetite. Such association of minerals is known in SW Spain (Jiménez-Millán and Velilla 1998), in the Eastern Carpathians of Romania (Hirtopanu and Scott 1999), in Chvaletice deposit in Czech republic (•ák 1972), in Ural in Russia (Gerasimov et al. 1999) and in China (Zeng and Liu 1999).

Mn-silicates (rhodonite, pyroxmangite, anthophyllite), pyrophanite and magnetite are enclosed and cut by veinlets of distinctly younger sulphides (pyrite, chalcopyrite and pyrrhotite). Presence of Ni, Co, and Cu minerals like pentlandite, chalcopyrite and cobaltite may reflect adsorption of these elements in the former sedimentary – diagenetic manganese minerals. Mn-rich calcite and quartz accompany the hydrothermal phase.

The volcanic-sedimentary manganese ores with the shale – – chert spilite formation and high content of Fe are closely related to residual fluids of juvenile basalt provenance (Borchert 1980). Relatively high contents of iron reflect presence of iron hydroxides and Mn-rich magnetite in the studied samples. However, Mn contents are dominant and chert spilite formation is absent at Čučma and Malá Hekerová deposits. The volcanic-

sedimentary sedex sulphide deposits occur in the Gemericum Superunit (Smolník, Mníšek and Bystrý Potok) and they are accompanied by insignificant accumulation of iron oxides. Volcanic source of manganese can not be excluded but recent data suggest that diagenetic processes with active involvement of organic matter took more important part in the precipitation of manganese in the studied area.

Characteristic feature of deposits is metamorphic association of manganese minerals. Rhodonite-pyroxmangite geothermometer of Mn-ore from Čučma gives 375 °C (Faryad 1991) and 390 °C (Rojkovič 1999; according Schultz-Güttler and Peters 1987). P-T-XCO2 conditions of metamorphism, according recent data of Faryad (1994), correspond to 400-420 °C for 350 MPa and X_{CO2} 0.05-0.06. Metamorphosed silicate-carbonate manganese rocks were replaced by Mn oxides and hydroxides (mainly todorokite and pyrolusite) during supergene processes in oxidation zone.

Conclusions

1. The Early Palaeozoic black phyllites of the Gemericum Superunit represent metamorphosed black shales rich in organic matter. Microbial suboxic diagenesis and reduction of precipitated MnO_2 formed Mn carbonates in sediments with clay minerals and quartz.
2. Manganese carbonate-silicate rock were metamorphosed into queluzite with the association: rhodonite, rhodochrosite, tephroite, spessartite, anthophyllite, pyroxmangite, Mn-rich magnetite, pyrophanite, muscovite, manganpyrosmalite , albite, rutile and allanite-(Ce).
3. Subsequent hydrothermal association is represented by Mn-rich calcite, pyrite, pentlandite, sphalerite, chalcopyrite, pyrrhotite, cobaltite, ullmannite, galena, chlorite, bementite and quartz.
4. Todorokite, pyrolusite, cryptomelane, goethite and "limonite" have been formed during supergene processes through oxidation of the previous association of minerals.

Acknowledgement

WDX and EDX analysis were carried out in the Geological Survey of Slovak Republic in Bratislava by P. Siman and P. Konečný. XDA was made in the Geological Institute of the Slovak Academy of Sciences, Bratislava by Ľ. Puškelová. The study was partly supported by VEGA Project # 1/7293/20.

References

BORCHERT H., 1980. On the genesis of manganese ore deposits. In: VARENTSOV I. M. and GRASSELY G. (Editors), Geology and geochemistry of manganese, Akadémiai Kiadó, Budapest, Volume II, pp. 13-44.

CORBIN J.-C., PERSON A., IATZOURA A., FERRÉ B. and RENARD M., 2000. Manganese in Pelagic carbonates: indication of major Tectonic events during the geodynamic evolution of a passive continental margin (the Jurassic European Margin of the Tethys-Ligurian Sea). *PALAEO, Paleogeography, Paleoclimatology, Paleoecology*, 156: 123-138.

FARYAD S. W., 1991. Metamorphism of the Early Palaeozoic sedimentary rocks in Gemericum. *Mineralia Slov.*, 23: 315-324 (in Slovak).

FARYAD S. W., 1994. Mineralogy of Mn-rich rocks from greenschist facies suquences of the Gemericum, West Carpathians, Slovakia. *N. Jb. Miner. Mh. Jg.*: 464-480.

FORCE E. R. and CANNON W. F., 1988. Depositional Model for Shallow-Marine Manganese. Deposits around Black Shale Basins. *Econ. Geol.*, 83: 93-117.

GERASIMOV N.N., NASEDKINA V.K., ONISHCHENKO S.A. and SHISHKIN M.A., 1999. Mineral composition of ores of the Parnok ferromanganese deposit (Polar Urals, Russia). *Geol. Ore Deposits*, 41: 73-84.

GRECULA P., ABONYI A., ABONYIOVÁ M., ANTAŠ J., BARTALSKÝ B., BARTALSKÝ J., DIANIŠKA I., DRNZÍK E., ĎUĎA R., GARGULÁK M., GAZDAČKO Ľ., HUDÁČEK J., KOBULSKÝ J., LÖRINCZ L., MACKO J., NÁVESŇÁK D., NÉMETH Z., NOVOTNÝ L., RADVANEC M., ROJKOVIČ I., ROZLO•NÍK L., ROZLO•NÍK O., VARČEK C. and ZLOCHA J., 1995. Mineral deposits of the Slovak Ore Mountains. Vol. 1, Geocomplex, Bratislava.

GUTZMER J. and BEUKES N. J., 1998. The manganese formation of the Neoproterozoic Penganga Group, India – revision of an enigma. *Econ. Geol.*, 93: 1091-1102.

HIRTOPANU P. and SCOTT P. W., 1999. Mineralogy and genesis of metamorphic manganese deposits from Bistrita Mountains, Eastern Carpathians, Romania. In: STANLEY C.J. et al. (Editors.), Mineral Deposits: Processes to Processing, Balkena, Rotterdam.

HUCKRIEDE H. and MEISCHNER D., 1996. Origin and environment of manganese-rich sediments within black-shale basins. *Geochim. Cosmochim. Acta*, 60: 1399-1413.

JIMÉNEZ-MILLÁN J. and VELILLA N., 1998. Mn-Fe spinels and silicates in maganese-rich rocks from the Ossa-Morena Zone, southern Iberian massif, southwestern Spain. *Can. Mineral.*, 36: 701-711.

KANTOR J., 1954. Origin of manganese ore in Spišsko-gemerské rudohorie Mts. *Geol. Práce, Zpr.*, 1: 70-71 (in Slovak).

MADERSPACH L., 1880. Magyarország vasérczfekhelyei. Budapest.

OKITA P. M., 1992. Manganese Carbonate Mineralization in the Molango District, Mexico. Econ. Geol., 87, 1345-1366.

ÖZTÜRK H. and FRAKES L. A., 1995. Sedimentation and diagenesis of an Oligocene manganese deposit in a shallow subbasin of the Paratethys: Thrace Basin, Turkey. *Ore Geology Rev.*, 10: 117-132.

ÖZTRÜK H. and HEIN J. R., 1997. Minaralogy and stable isotopes of black shale hosted manganese ores, Southwestern Taurides, Turkey. *Econ. Geol.*, 92: 733-744.

PAPP K.V., 1915. A Magyar birodalom vasérc és köszénkészlete. A Fraklin-társulat nyomdája, Budapest.

REDFERN S.A.T., KNIGHT K.S., HENDERSON C.M.B. and WOOD B.J., 1998. Fe-Mn cation ordering in fayalite-tephroite $(Fe_xMn_{1-x})_2SiO_4$ olivines: a neutron diffraction study. *Mineral. Mag.*, 62: 607-615.

ROJKOVIČ I., 1999. Manganese mineralization in the Western Carpathians, Slovakia. *Geol. Carpath.*, 50: 191-192.

ROJKOVIČ I. and KHUN M., 1997. Metamorphosed Paleozoic black shales in the Western Carpathians, Slovakia. Mineral Deposits, Balkema, Rotterdam, pp. 103-106.

ROJKOVIČ I., PUŠKELOVÁ Ľ., KHUN M. and MEDVEĎ J., 1995. U-REE-Au in veins and black shales of the Gemericum, Slovakia. In: PAŠAVA J., KŘÍBEK B., •ÁK K., (editors), Mineral deposits: from their origin to their environmental impacts. A. A. Balkema, Rotterdam, Brookfield. pp. 789-792.

ROY S., 1980. Genesis of sedimentary manganese formations: Processes and products in recent and older geological ages.

In: VARENTSOV I. M. and GRASSELY G. (Editors), Geology and geochemistry of manganese, Akadémiai Kiadó, Budapest, Volume II, pp. 13-44.

ROY S., 1992. Environments and Processes of Manganese Deposition. *Econ. Geol.*, 87: 1218-1236.

SCHULTZ-GÜTTLER R. and PETERS T., 1987. Coexisting rhodonite and pyroxmangite in the system MnSiO3 – CaSiO3 – MgSiO3 – FeSiO3 as a geothermometer. Schweiz. *Miner. Petrogr. Mitt.*, 67: 47-51.

TANG S.Y. and LIU T.B., 1999. Origin of the early Sinian Minle manganese deposit, Hunan Province, China. *Ore Geol. Rev.*, 15: 71-78.

ZENG Y. Y. and LIU T. B., 1999. Characteristics of the Devonian Xialei manganese deposit, Guangxi Zhuang Autonomous Region, China. *Ore Geol. Rev.*, 15: 153-163.

• Á K L., 1972. Metamorphic paragenesis of the manganese-pyrite horizon in the •elezné hory Mts. (Bohemia). *Čas. Mineral. Geol.*, 17: 345-356.